THE JOURNAL OF PHYSICAL CHEMISTRY C LETTERS

2007, *111,* 10162−10165
Published on Web 06/20/2007

Position-Controlled Seedless Growth of ZnO Nanorod Arrays on a Polymer Substrate via Wet Chemical Synthesis

Benjamin Weintraub,[†] Yulin Deng,*[,‡] and Zhong L. Wang*[,†]

School of Materials Science and Engineering, and School of Chemical and Biomolecular Engineering, Georgia Institute of Technology, Atlanta, Georgia 30332-0245

Received: May 16, 2007; In Final Form: June 8, 2007

A novel wet chemical technique for the site-selective growth of ZnO nanorod arrays on polymer substrates is described. Electron beam lithography is employed to define nanorod positions using a polymethylmethacrylate (PMMA) mask on a Kapton polyimide substrate with a Au intermediate layer. An applied potential is utilized to enhance the nucleation process and achieve ZnO nanorods with a base diameter of 200 nm. The technique does not require a ZnO seed layer and can be carried out at temperatures as low as 70 °C. Structural characterization of the as-grown ZnO nanorods has been investigated by scanning electron microscopy and X-ray diffraction. This technique represents a new low-cost method for integrating ZnO nanorods into flexible electronic devices.

Recently, there has been growing interest in ZnO nanorod arrays for applications in electronics and optoelectronics such as solar cells,[1] UV lasers,[2] nanogenerators,[3,4] light emitting diodes,[5] and field emission devices.[6] One-dimensional ZnO nanostructured arrays are typically synthesized in the gas phase catalytically using the vapor−liquid−solid process[7] on single-crystal sapphire substrates and catalyst-free using metal−organic chemical vapor deposition (MOCVD).[8,9] These methods produce high-quality single-crystal nanorods but have strict substrate requirements due to the high synthesis temperature requirements (450−900 °C) and are limited by sample uniformity. Wet chemical methods are an attractive alternative since they can be carried out at temperatures as low as 50 °C and allow for a greater variety of crystalline and amorphous substrates.[10,11,12]

Wet chemical growth can be achieved independent of the substrate by employing ZnO seeds in the form of thin films or nanoparticles. This approach typically requires higher temperature substrate processing. ZnO seeds must be annealed at 150 °C to improve particle adhesion to the substrate, and ZnO nanorod vertical alignment could be further improved by textured ZnO seeds annealed at 350 °C.[13,14] However, there is interest in carrying out the entire process from substrate preparation to synthesis at low temperatures, which would be compatible with organic substrates for applications in flexible and wearable electronics. ZnO nanorod arrays have been synthesized on polymer substrates such as polydimethylsiloxane (PDMS), Au-coated Kapton, and polycarbonate coated with polystyrene beads.[12,14,15] As expected, the nanorods grow at random sites on the substrate surface.

Site-selective growth of ZnO nanorods is of interest for the integration of nanostructures into MEMS and NEMS devices. Nanosphere lithography has been employed to define Au catalyst patterns for ZnO nanowire arrays on single-crystal sapphire.[16] Electron beam lithography was successfully utilized to define position and size-controlled micro- and nanorod arrays on Si substrates covered with a ZnO thin film seed layer.[17] Photolithography techniques have been used to pattern micron-size regions and enhance the growth with ZnO nanoparticle seeds.[18] Microstamped self-assembled monolayers (SAM) have also been employed to define ZnO micron-size patterned arrays.[19]

In this Letter, we report the site-selective growth of individual ZnO nanorods in patterned arrays by a wet chemical approach on organic substrates. This novel synthesis technique does not require a ZnO thin film or nanoparticle seeds, and it can be carried out at low temperatures (<70 °C), making it an important synthesis technique for flexible electronic applications.

The following process flow employed electron beam lithography to define the nanorod positions and an applied potential across the substrate relative to a second reference electrode to enhance the ZnO nucleation. Figure 1 details the process flow. The substrate was a 50 μm thick Kapton polyimide film provided by DuPont (HN200). A thin layer of Au was thermally evaporated (0.3 Å/s deposition rate, 50 nm) to provide electrical conductivity and uniform nucleation sites on the substrate. The substrate was then spin coated with 2% 495,000 M_w PMMA resist in anisole at 2000 rpm for 45 s, resulting in a thickness ca. 75 nm. Finally, the substrate was baked on a hot plate at 180 °C for 90 s to remove the solvent. Arrays of circular patterns (diameters of 200 nm and 1−9 μm) were patterned into the resist using a LEO 1550 field emission scanning electron microscope (FESEM) modified with a J.C. Nabity nanometer pattern generation system (NPGS). The substrates were developed in a 3:1 by volume isopropyl alcohol/methyl isobutyl ketone solution to reveal the patterned features. Electrical contact was made to the substrate by selectively removing a small portion of the PMMA resist using acetone.

* To whom correspondence should be addressed. E-mail: zlwang@gatech.edu (ZLW); Yulin.Deng@ipst.gatech.edu (YLD).
[†] School of Materials Science and Engineering.
[‡] School of Chemical and Biomolecular Engineering.

10.1021/jp073806v CCC: $37.00

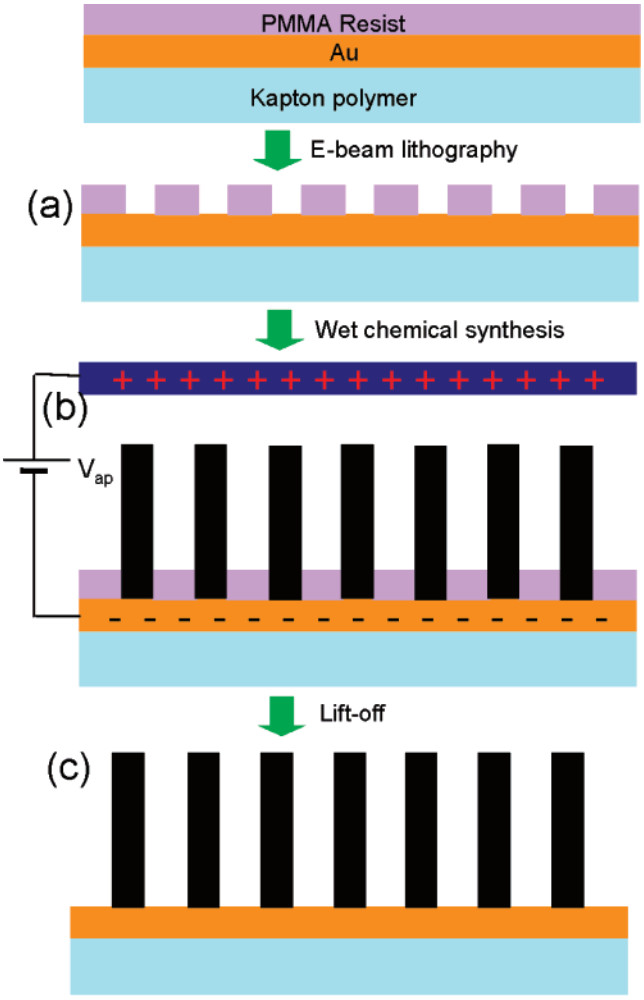

Figure 1. Process flow for lithography-based density-controlled ZnO nanorod array growth. Flexible Kapton polymer substrate is coated in a Au thin film and PMMA resist. (a) Desired density is defined using electron beam lithography, and the Au pattern is subsequently exposed during the developing step. (b) The patterned substrate is immersed in a nutrient solution bath and held at a −500 mV bias relative to the reference electrode. (c) The PMMA resist is finally removed in the lift-off step.

The patterned substrate was submerged vertically into a nutrient solution parallel to a second Au-coated Kapton substrate of equal dimensions, referred to as the reference electrode. A −500 mV potential was applied relative to the patterned substrate using a Hewlett−Packard DC power supply (Model E3620A). The aqueous nutrient solution was composed of 20 mM zinc nitrate hexahydrate and 20 mM hexaminetetramine (HMTA) and maintained at 70 ± 5 °C on a hot plate. All chemicals were reagent grade and purchased from Fluka. The reaction time was varied between 1 and 5 h in order to control the nanorod length.

Once the synthesis was complete, the PMMA resist was removed with acetone and the sample was rinsed with DI water and air-dried overnight. The as-grown nanorods were characterized by a LEO 1530 FESEM operated at an accelerating voltage of 5 kV. X-ray diffraction data was collected on a PANalytical X-Pert Pro Alpha-1 with Cu Kα radiation.

Our process technique enabled position control of ZnO nanorods of micron- and submicron-sized patterns. Figure 2a demonstrates micron scale patterning of 5 × 5 arrays with circular patterns ranging in diameter from 1 to 9 μm in micron step sizes. The largest diameter array of 9 μm is shown in Figure 2b. The nanorods range in diameter from 50 to 150 nm and

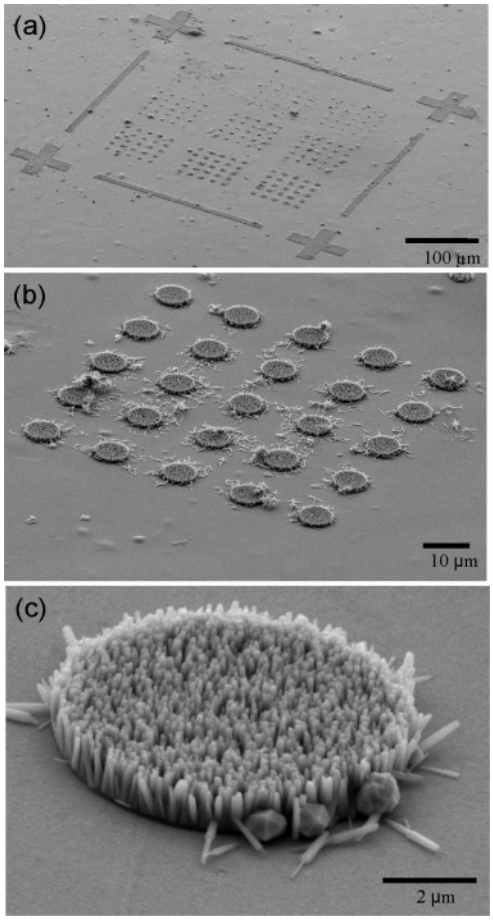

Figure 2. SEM images of micron-scale ZnO nanorod patterns of 5 × 5 arrays. (a) Low-magnification tilted SEM image of ZnO nanorod arrays ranging in diameter from 1 to 9 μm. (b) Tilted SEM image of a patterned ZnO nanorod array with a 9 μm circular diameter. (c) High-magnification tilted SEM image of a single patterned ZnO nanorod array with a 9 μm circular diameter.

have a uniform length of 1.4 μm. The nanorods exhibited a high degree of vertical alignment and growth density while fully occupying the patterned regions, as can be seen in Figure 2c. A small amount of nonvertical growth was observed at the resist mask boundaries.

In addition, submicron-sized patterns were defined for growth of single ZnO nanorod arrays. Figure 3a shows a low magnification SEM image of a 25 × 25 array of individual ZnO nanorods separated by 1.25 μm. Circular patterns of 200 nm were defined in the resist in order to nucleate a single ZnO nanorod. ZnO nanorods did not grow on the PMMA resist regions due to a lack of nucleation sites.[17] It was found that 200 nm was the optimum circular diameter in order to nucleate a single nanorod under the given experimental conditions. At 70 °C, the approximate growth rate was 0.7 μm/h. The nanorod length was controlled by the synthesis time. Figure 3b shows a high-magnification SEM image of the ZnO nanorod array profile. Figure 3c shows a top SEM image of the array and demonstrates that the nanorods exhibit a high degree of vertical alignment. The base diameter was defined by the resist mask. Above the resist, lateral growth occurred along the nonpolar $\{1\bar{1}00\}$ facets, resulting in nanorods with a diameter of 200 ± 50 nm.

The ability to scale up the patterned growth to larger array sizes and densities has also been demonstrated. Figure 4a shows a SEM image of a 50 × 50 array of single ZnO nanorods separated by a distance of 0.5 μm. The lengths ranged from

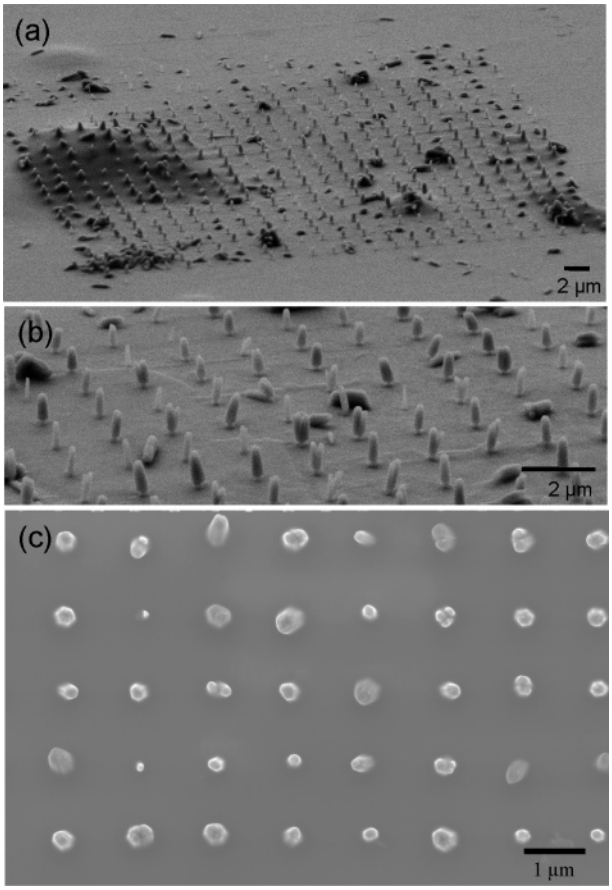

Figure 3. SEM image of a 25 × 25 array of patterned single ZnO nanorods with a spacing of 1.25 μm. (a) Low-magnification SEM image at a 70° stage tilt of a ZnO nanorod array. (b) Higher magnification SEM image of the array. (c) Top view SEM image of the array.

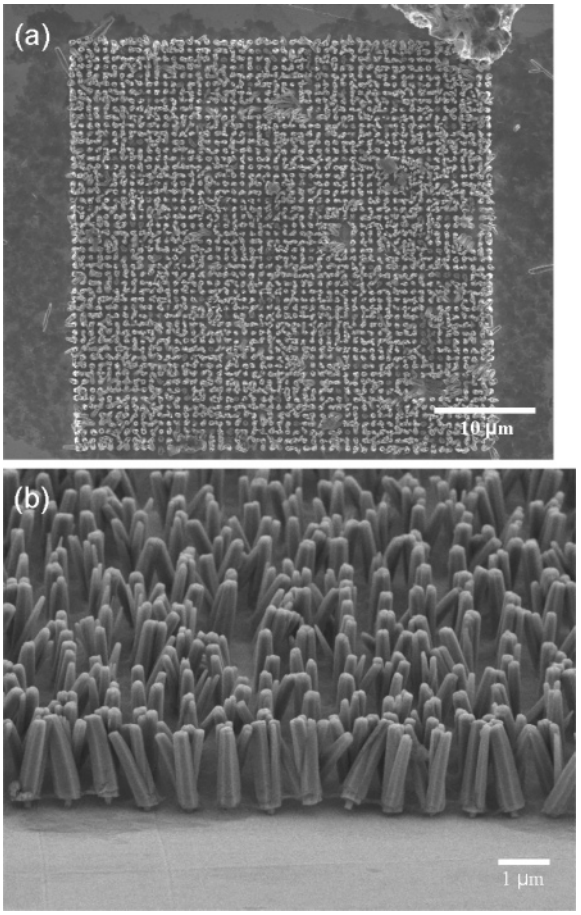

Figure 4. SEM image of a 50 × 50 array of patterned single ZnO nanorods with a spacing of 0.5 μm. (a) Top view SEM image of the array. (b) SEM image of the nanorod array at a 60° stage tilt.

1.8 to 2.0 μm, and some lateral growth can be seen in the SEM profile image in Figure 4b. The base width was 200 nm, as defined by the resist pattern, and the upper diameter ranged from 300 to 400 nm. The lateral growth caused some of the nanorods to detach from the substrate.

After systematically varying the diameter of the patterned circular features, it was found that nucleation could not be achieved within smaller pattern sizes (<1 μm) without an applied potential. The nucleation process was hampered since there were fewer nucleation sites exposed on the Au. It has been found that an applied potential increases the nucleation density of ZnO nanorods by up to 4 orders of magnitude on polished surfaces.[20] The applied potential was essential for achieving high-density nucleation within the micron-sized patterns and single nanorod nucleation in the 200 nm diameter patterns.

ZnO nanostructures form by the hydrolysis of zinc nitrate in water in the presence of HMTA. The detailed role of HMTA is still under investigation. HMTA is a nonionic cyclic tertiary amine that can act as a Lewis base with metal ions and a bidentate ligand capable of bridging two zinc(II) ions in solution.[21] HMTA can also hydrolyze to produce formaldehyde and ammonia under the given reaction conditions.[22] It is thought to gradually decompose and provide a steady supply of ammonia, which can form ammonium hydroxide and complex with zinc(II) to form $Zn(NH_3)_4^{2+}$.[23,24] Zinc(II) is known to coordinate in tetrahedral complexes. Under the given pH and temperature, zinc(II) is thought to exist primarily as $Zn(OH)_4^{2-}$ and $Zn(NH_3)_4^{2+}$. The ZnO is formed by the dehydration of these intermediates. Although the system is quite complex, we represent the dominant chemical reactions on the basis of our analysis and that of others[24−28] by the following formulas

$$C_6H_{12}N_4 + 6H_2O \leftrightarrow 6CH_2O + 4NH_3 \quad (1)$$

$$C_6H_{12}N_4 + Zn^{2+} \rightarrow [Zn(C_6H_{12}N_4)]^{2+} \quad (2)$$

$$NH_3 + H_2O \leftrightarrow NH_4^+ + OH^- \quad (3)$$

$$Zn^{2+} + 4NH_3 \rightarrow Zn(NH_3)_4^{2+} \quad (4)$$

$$Zn^{2+} + 4OH^- \rightarrow Zn(OH)_4^{2-} \quad (5)$$

$$Zn(NH_3)_4^{2+} + 2OH^- \rightarrow ZnO + 4NH_3 + H_2O \quad (6)$$

$$Zn(OH)_4^{2-} \rightarrow ZnO + H_2O + 2OH^- \quad (7)$$

$$[Zn(C_6H_{12}N_4)]^{2+} + 2OH^- \rightarrow ZnO + H_2O + C_6H_{12}N_4 \quad (8)$$

After analysis of the dominant chemical reactions in the system, the role of the applied potential is more apparent. Positively charged intermediates are formed in reactions 2 and 4. The electric field established between the patterned substrate and the reference electrode caused the $Zn(NH_3)_4^{2+}$ and $[Zn(C_6H_{12}N_4)]^{2+}$ intermediates to migrate toward the negatively biased patterned substrate. This caused a high concentration of the ZnO precursors to become localized at the patterned substrate region. Thus, enhanced nucleation could be achieved in the

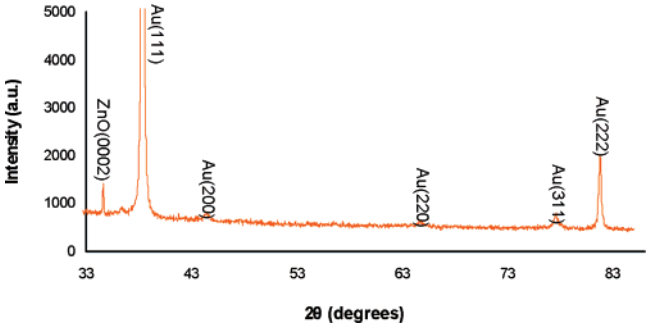

Figure 5. X-ray diffraction data for the patterned ZnO nanorod array.

submicron space-confined regions. Others[20,29−32] have proposed that the applied potential causes an increased OH^- concentration by the reduction of NO_3^- in an electrochemical reaction at the negative electrode. As such, the reaction would proceed as follows

$$NO_3^- + H_2O + 2e^- \rightarrow NO_2^- + 2OH^- \quad (9)$$

$$Zn^{2+} + 2OH^- \rightarrow ZnO + H_2O \quad (10)$$

Both mechanisms involve an increased precursor concentration at the patterned substrate, and further investigation is required to determine which is more dominant.

X-ray diffraction data shown in Figure 5 shows the data for the patterned substrate. The appearance of the (0002) peak at 34.6° confirms the [0001] as the fast growth direction and the high degree of vertical alignment. It also confirms the crystallinity of the nanorods. The strong intensity of the Au peaks diminishes the intensity of the (0004) peak at 72.5°.

In summary, a new synthesis technique has been demonstrated for growing ZnO nanorods site-selectively on a polymer substrate. The synthesis does not require the use of ZnO seeds and has been demonstrated at temperatures as low as 70 °C. The technique utilizes electron beam lithography to define the specific nanorod positions and an applied potential to enhance the nucleation process. In terms of electronic device integration, the nanorods are already in electrical contact with the Au thin film, and if left remaining, the PMMA resist can serve as an insulating layer. This technique represents a novel and low-cost way for integrating ZnO nanorods into flexible electronic and piezoelectronic[33] devices.

Acknowledgment. B.W. thanks the Institute of Paper Science and Technology for the fellowship.

References and Notes

(1) Law, M.; Greene, L. E.; Johnson, J. C.; Saykally, R.; Yang, P. D. *Nat. Mater*. **2005**, *4*, 455.
(2) Huang, M. H.; Mao, S.; Feick, H.; Yan, H. Q.; Wu, Y. Y.; Kind, H.; Weber, E.; Russo, R.; Yang, P. D. *Science* **2001**, *292*, 1897.
(3) Wang, X. D.; Song, J. H.; Liu, J.; Wang, Z. L. *Science* **2007**, *316*, 102.
(4) Wang, Z. L.; Song, J. H. *Science* **2006**, *14*, 242.
(5) Saito, N.; Haneda, H.; Sekiguchi, T.; Ohashi, N.; Sakaguchi, I.; Koumoto, K. *Adv. Mater*. **2002**, *12*, 418.
(6) Cui, J.; Daghlian, C. P.; Gibson, U.; Pusche, R.; Geithner, P.; Ley, L. *J. Appl. Phys*. **2005**, *97*, 044315.
(7) Yang, P. D.; Yan, H. Q.; Mao, S.; Russo, R.; Johnson, J.; Saykally, R.; Morris, N.; Pham, J.; He, R. R.; Choi, H. J. *Adv. Funct. Mater*. **2002**, *12*, 323.
(8) Park, W. I.; Yi, G. C.; Kim, M. Y.; Pennycook, S. J. *Adv. Mater.* **2002**, *14*, 1841.
(9) Wu, J. J.; Liu, S. C. *Adv. Mater.* **2002**, *14*, 215.
(10) Vayssieres, L. *Adv. Mater*. **2003**, *15*, 464.
(11) Vayssieres, L.; Keis, K.; Lindquist, S. E.; Hagfeldt, A. *J. Phys. Chem. B* **2001**, *105*, 3350.
(12) Lin, C. C.; Chen, S. Y.; Cheng, S. Y. *J. Cryst. Growth* **2005**, *283*, 141.
(13) Greene, L.; Law, M.; Tan, D. H.; Montano, M.; Goldberger, J.; Somorjai, G.; Yang, P. D. *Nano Lett.* **2005**, *5*, 1231.
(14) Greene, L. E.; Law, M.; Goldberger, J.; Kim, F.; Johnson, J. C.; Zhang, Y. F.; Saykally, R. J.; Yang, P. D. *Angew. Chem., Int. Ed*. **2003**, *42*, 3031.
(15) Gao, P.; Song, J. H.; Liu, J.; Wang, Z. L. *Adv. Mater*. **2007**, *19*, 67.
(16) Wang, X. D.; Summers, C. J.; Wang, Z. L. *Nano Lett.* **2004**, *4*, 423.
(17) Kim, Y. J.; Lee, C. H.; Hong, Y. J.; Yi, G. C.; Kim, S. S.; Cheong, H. *Appl. Phys. Lett*. **2006**, *89*, 163128.
(18) Kang, B. S.; Pearton, S. J.; Ren, F. *Appl. Phys. Lett.* **2007**, *90*, 083104.
(19) Sounart, T.; Liu, J.; Voigt, J.; Hsu, J.; Spoerke, E.; Tian, Z. R.; Jiang, Y. *Adv. Funct. Mater*. **2006**, *16*, 335.
(20) Cui, J.; Gibson, U. *J. Phys. Chem. B* **2005**, *109*, 22074.
(21) Ahuja, I. S.; Yadava, C. L.; Singh, R. J. *Mol. Struct.* **1982**, *81*, 229.
(22) Strom, J. G.; Jun, H. W. *J. Pharm. Sci.* **1980**, *69*, 1261.
(23) Govender, K.; Boyle, D. S.; Kenway, P. B.; O'Brien, P. *J. Mater. Chem.* **2004**, *14*, 2575.
(24) Wang, Z.; Qian, X. F.; Yin, J.; Zhu, Z. K. *Langmuir* **2004**, *20*, 3441.
(25) Yu, L.; Zhang, G.; Li, S.; Xi, Z.; Guo, D. *J. Cryst. Growth* **2007**, *299*, 184.
(26) Zhang, J.; Sun, L. D.; Yin, J. L.; Su, H. L.; Liao, C. S.; Yan, C. H. *Chem. Mater*. **2002**, *14*, 4172.
(27) Zhang, J.; Sun, L. D.; Liao, C. S.; Yan, C. H. *Chem. Commun*. **2002**, 262.
(28) Wang, Z.; Qian, X. F.; Yin, J.; Zhu, Z. K. *J. Solid State Chem*. **2004**, *177*, 2144.
(29) Izaki, M.; Omi, T. *J. Electrochem. Soc*. **1996**, *143*, L53.
(30) Chatterjee, A.; Foord, J. *Diamond Relat. Mater*. **2006**, *15*, 664.
(31) Cao, B. Q.; Cai, W. P.; Sun, F. Q.; Li, Y.; Lei, Y.; Zhang, L. D. *Chem. Commun*. **2004**, 1604.
(32) Cao, B. Q.; Li, Y.; Duan, G. T.; Cai, W. P. *Cryst. Growth Des*. **2006**, *6*, 1091.
(33) Wang, Z. L. *Mater. Today* **2007**, *10*, 20.